UC Irvine
UC Irvine Previously Published Works

Title

Chemically Tuned Intracellular Gene Delivery by Core-Shell Nanoparticles: Effects of Proton Buffering, Acid Degradability, and Membrane Disruption

Permalink

https://escholarship.org/uc/item/4v11n95q

Journal

ChemMedChem, 17(7)

ISSN

1860-7179

Authors

Cho, Soo Kyung
Lee, Rebecca T
Hwang, Yoon-Hwae
et al.

Publication Date

2022-04-05

DOI

10.1002/cmdc.202100718

Peer reviewed

Chemically Tuned Intracellular Gene Delivery by Core-Shell Nanoparticles: Effects of Proton Buffering, Acid Degradability, and Membrane Disruption

Soo Kyung Cho[b], **Rebecca T. Lee**[c], **Yoon-Hwae Hwang**[d], **Young Jik Kwon**[a]

[a]Departments of Pharmaceutical Science, Chemical and Biomolecular Engineering, Biomedical Engineering, and Molecular Biology and Biochemistry University of California, Irvine, 132 Sprague Hall, Irvine, CA 92697-3958 (USA)

[b]Crystal Bank PNU, Pusan National University, 2222 Nano Building, Samnangjin-ro, Miryang, Gyeongsangnam-do 50463 (Republic of Korea)

[c]Department of Biomedical Engineering and Medical Scientist Training Program, University of California, Irvine, B200 Sprague Hall, Irvine, CA 92697-3958 (USA)

[d]Department of Nano Energy Engineering, Pusan National University, Pusandaehak-ro 63 beon-gil 2, Jangjeon-dong, Geumjung-gu, Busan 46241 (Republic of Korea)

Abstract

Nanoparticles consisting of a condensed nucleic acid core surrounded by protective layers which aid to overcome extracellular and intracellular hurdles to gene delivery (i.e., core-shell nanoparticles, CSNPs) synthetically mimic viruses. The outer shells shield the core and are particularly designed to enable facilitated release of the gene payload into the cytoplasm, the major limiting step in intracellular gene delivery. The hypothetical proton sponge effect and degradability in response to a stimulus (i.e., mildly acidic pH in the endosome) are two prevailing, although contested, principles in designing effective carriers for intracellular gene delivery via endosomal escape. Utilizing the highly flexible chemical-tuning of the polymeric shell via surface-initiated photo-polymerization of the various monomers at different molecular ratios, the effects of proton buffering capacity, acid-degradability, and endosomal membrane-lysis property on intracellular delivery of plasmid DNA by CSNPs were investigated. This study demonstrated the equivalently critical roles of proton buffering and acid-degradability in achieving efficient intracellular gene delivery, independent of cellular uptake. Extended proton buffering resulted in further improved transfection as long as the core structure was not compromised. The results of the study present a promising synthetic strategy to the development of an efficient, chemically-tunable gene delivery carrier.

kwonyj@uci.edu, sookyungcho@pusan.ac.kr.

Keywords

Core-shell nanoparticles; gene delivery; proton sponge; acid-degradability; structure-activity relationship

Introduction

Gene therapy is a promising emerging therapeutic modality.[1] Among the numerous extracellular and intracellular impediments to efficient gene delivery, cytosolic release of nucleic acids prior to premature inactivation in the digestive endosome/lysosome, acts as the major limiting step.[2] In attempts to tackle this pivotal challenge, synthetic gene delivery carriers, commonly called nonviral vectors, have been developed by employing various materials including polymers and lipids.[3] However, the limited and often contradictory mechanistic understanding of the key factors that facilitate endosomal escape makes the design of efficient nonviral vectors challenging.[4] The most widely used approach is to harness the mildly acidic environment in the endosome and lysosome. Two actively researched design principles in nonviral gene delivery are proton sponge effect and acid-degradability.[5] The proton sponge effect hypothesizes an influx of anions (e.g., Cl^-) and water to the endosome/lysosome in order to compensate the proton influx via proton pump driven by the protonation of the amines of nonviral vectors.[5a] This phenomenon is speculated to eventually lead to osmotic swelling, endosomal membrane rupture, and finally release of nucleic acids into the cytoplasm. However, the proton sponge effect hypothesis was scrutinized when a remote correlation between intracellular release and the proton buffering capacity of nonviral vectors was observed.[6] Another synthetic strategy in nonviral gene delivery that is particularly popular is disruption of the endosome/lysosome by the generation of fragmented molecules and rapid structural changes of nonviral vectors upon acid-degradation.[7] With both approaches, the genetic payloads are desirably kept in a condensed, protected form.

Many viruses are equipped with a core that encapsulates its genetic material (e.g., RNA and DNA) and ancillary molecules (e.g., enzymes for replication and incorporation to the host) and capsid or envelope that not only protects the core but also dictates cellular entry and cytosolic release.[8] In an attempt to synthetically mimic such viruses, we previously developed a core-shell nanoparticle (CSNP) platform comprising of a nucleic acid-complexing core and cationic acid-degradable polymeric shell.[9] These CSNPs can accommodate a variety of different cores as desired, including polyplexes of cationic polymer (e.g., PEI and cationic polypeptides), small cationic molecules (e.g., spermine), or even viral particles (e.g. adenovirus and AAV). The polymeric shell of these CSNPs are chemically engineered via surface-initiated photo-polymerization of monomers and cross-linkers at desired ratios to enable tuning of properties such as endosomal escape, proton buffering capacity, and membrane-disruption which are independent of the nucleic acid-containing core.[10]

In this study, the polymeric shell of CSNPs were synthesized with 1°, 2°, and 3° amine-, imidazole-, and/or Triton X-100-bearing monomers, along with acid-degradable or non-

degradable cross-linkers via surface-initiated photo-polymerization at a desired mixture. Utilizing the high synthetic flexibility of the CSNPs, this study demonstrated the multi-dimensional effects of proton buffering, acid-degradability, and membrane disruption on intracellular release of the nucleic acid payload and transfection efficacy. This study offers insights in designing an efficient gene delivery carrier by incorporating monomers and crosslinkers with a broad range of molecular properties.

Results and Discussion

Synthesis of CSNPs with chemically tunable proton buffering, acid-degradability, and membrane disruption capabilities

Our CSNPs with a condensed nucleic acid core and a highly tunable polymeric shell for varying molecular properties are well suited for facile and highly controlled studies of chemical structure-transfection activity relationships. CSNPs were synthesized via photo-polymerization of various monomers on the surface of protamine sulfate (PS)/plasmid DNA (pDNA) polyplexes (Figure 1). PS/pDNA polyplexes were chosen due to their efficient transnuclear transport capability as demonstrated in the previous study.[9a] Briefly, the photo-initiator eosin-Y-conjugated PS was used to complex pDNA to prepare PS/pDNA polyplexes (70 nm in diameter).[11] Monomers and crosslinkers with varying molecular properties of proton buffering, acid-degradability, and membrane disruption capability were photo-polymerized by visual light irradiation in the presence of ascorbic acid as a catalyst. This method allows readily tuned CSNP size, surface charge, degradability, and buffering capacity that altogether dictates transfection efficiency by polymerizing the mixture of different monomers and crosslinkers at a desired molecular ratio. Acid-degradable monomers with primary amine (1°), secondary amine (2°), tertiary amine (3°), and imidazole (Im) terminus were prepared to study the effect of proton buffering on endosomal escape and transfection efficacy, as well as the facilitated cellular internalization of cationic particulates. Additionally, Im monomer was included for its distinctive buffering profile at mildly acidic pH in the endosomal compartment.

Acid-base titration was performed to study the ability of the cationic monomers to be protonated and serve as a proton buffer for a drop in pH from 11 to 2 (Figure 2). 1° and 3° monomers demonstrated a similar buffering profile which differed from that of 2° and Im (Figure 2A). 2° monomer exhibited the least buffering capacity in the tested pH range (Figure 2B). Im monomer had a distinctive titration profile from the rest of monomers, capable of buffering at the known endosomal pH range between 5 and 9[12] and its inclusion at 10% to 1° monomer (1°-10% Im) resulted in a broadened proton buffering capacity (Figure 2B). Nondegradable monomer with a primary amine terminus (ND1°) and nondegradable crosslinker (NDXL) were also synthesized to control the acid-degradability of CSNPs. In addition to assessing proton sponge and acid-degradability in endosomal escape of PS/pDNA core, an acid-degradable monomer with terminal Triton X-100 (TX) was prepared and incorporated into the polymeric shell of CSNPs to assess the hypothesis that the acid-cleavage of TX releases free Triton X-100 and facilitates endosomal escape (Figure 1). CSNPs with broader proton buffering (1°-Im) and combined proton buffering and membrane disruption (1°-TX) were readily prepared by adding additional monomer during

the surface-initiated photo-polymerization. The highly versatile and flexible synthesis of CSNPs is a promising tool to investigate the chemical structure and activity relationship and develop optimized nonviral gene delivery vectors.

Effect of different monomers on CSNP size, zeta potential, cellular uptake, and buffering capacity

Nanoparticle size, surface charge, degradability, and proton buffering capacity are key interwoven factors for achieving high transfection efficiency. Regardless of the varying chemical structures of the polymeric shell, all CSNPs synthesized under the conditions used in this study exhibited relatively similar sizes of around 250 nm in diameter (Figure 3A) with relatively low PDI (<0.3, individual data not shown). This comparatively uniform CSNP size allows for relatively direct comparison of the roles of the polymeric shell's chemical structure on cellular uptake and endosomal escape. When desired, CSNP sizes can be easily tuned by varying the concentrations of monomer and crosslinker and the polymerization conditions. Depending on the terminal amine structures of monomers, the zeta potential of CSNPs decreased in the order of $2° \approx 1° > 3° > \mathrm{Im}$ (Figure 3A), attributed to the lowered repulsive interactions by weaker cationic termini. Incorporation of Im monomers to 1° monomers reduced the zeta potential of CSNPs (+30 mV for 1° NP, + 28 mV for 1°-10% Im, and +14 mV for 1°-50% Im), without a change in size (Figure 3A). Adding 2% of neutral TX monomer reduced the CSNP size to around 200 nm and zeta potential to + 3 mV much lower than the other CSNPs (Figure 3A).

The cellular uptake of CSNPs by HeLa cells in general was closely related to the zeta potential, except for those made of 3° and Im monomers (Figure 3B). For example, CSNPs made of Im monomers, which had lower zeta potential than CSNPs made of 1° monomers showed lower cellular uptake. However, adding 10% and 50% Im monomers to 1° monomers lowered the zeta potential of CSNPs but increased the cellular uptake almost comparable to those of PEI and PS polyplex controls (Figure 3B). PEI and PS polyplexes are widely known for their high cellular uptake possibly due to high surface charge and small size. However, they also exhibit high cytotoxicity and low transfection efficiency, respectively. Effectively compensated by TX monomers for surface charge, the cellular uptake of CSNPs made of 1° and 2% TX monomers was greatly reduced. The addition of ND1° monomers to CSNPs slightly decreased cellular uptake, despite the higher surface charge, possibly due to unknown factors independent of zeta potential.

Intracellular localization of labeled pDNA was quantified to investigate its release from the endosome/lysosome (Figure 3C). HeLa cells were incubated with CSNPs for 4 h, washed and further incubated for additional 20 h. After lysosomes were stained, cells were imaged for escaped pDNA (green) and entrapped pDNA in the lysosome (yellow) and quantified for endosomal escape. This evaluation demonstrated that all CSNPs enabled the endosomal escape of the PS/pDNA polyplex core as aimed in our design. However, cytosolic pDNA release was not in a close alignment with proton buffering capacity. At 24 h, CSNPs made of 1°, 1°- 2% TX and 1°-10% Im monomers achieved >90% pDNA release, followed by those made of Im monomer (~80% release) (Figure 3C). CSNPs made of 3° monomer, which showed higher buffering capacity than those made of Im monomer, released pDNA less

efficiently than CSNPs made of 1° and Im monomers and even lower than those made of 2° monomer (Figure 3C). These results indicate that proton buffering is not the predominating factor governing endosomal escape, implicating the limitations of designing nonviral vector solely based on the proton sponge hypothesis. CSNPs made of ND1° monomer, which have the same proton buffering capacity as 1° monomer, showed pDNA release less than 50%, highlighting the indispensable roles of acid-degradability in endosomal escape (Figure 3C).

Determining the influence of acid-degradability and proton sponge effect on gene transfection by CSNPs

Transfection efficiency by the CSNPs made of monomers with different proton buffering capacities (1°, 2°, 3°, Im and 1°-10% Im) was found to be in the following order: 1°-10% Im > 1° > 2° ≈ Im > 3° (Figure 4A and B). This order was correlated neither to proton buffering nor pDNA release from the endosome/lysosome (Figure 3C). CSNPs made of 1° monomer enhanced the transfection compared to the PS/pDNA core and even the PEI/pDNA polyplex, but exhibited the highest cytotoxicity among the tested CSNPs (Figure 4C). The transfection by CSNPs made of 2° monomer was lower than that of CSNPs made of 1° monomer (Figure 4A and B), despite the similar zeta potential and cellular uptake (Figure 3). In contrast, CSNPs made of 2° monomer showed slightly improved cell viability, compared to that of CSNPs made of 1° monomer (Figure 4C). In addition, CSNPs made of 2° monomer showed higher zeta potential and cellular uptake than those of CSNPs made of Im monomer (Figure 3) but resulted in a comparable transfection efficiency (Figure 4A and B). With similar cellular uptake and proton buffering capacities, the transfection by CSNPs made of 3° monomer was significantly lower than that of CSNPs made of 1° monomer (Figure 4A and B). Due to the well-known high proton buffering capacity of tertiary amines, which are often exploited in polymers containing primary amines for improved proton buffering,[13] this drop in transfection efficiency suggests that the hypothetic proton sponge effect is not a fully reliable consideration in achieving efficient endosomal escape. The transfection by CSNPs made of Im monomer was lower than that of CSNPs made of 1° monomer but comparable to that of CSNPs made of 2° monomers (Figure 4A and B), while the buffering capacities of Im and 1° monomers was comparable but higher than that of 2° monomer (Figure 2). With the lower cellular uptake than that of CSNPs made of 2° monomer, CSNPs' comparable transfection efficiency implicates superior intracellular processes including endosomal escape. Addition of 10% Im monomer to 1° monomer substantially enhanced the transfection efficiency (Figure 4A and B). Though broadened buffering capacity in combination with improved cellular uptake speculatively contributed to the observation, higher release was not observed as anticipated (Figure 3C). The unclear correlation between transfection efficiency and proton buffering capacity suggests that proton sponge is not the sole factor behind successful transfection.

The effect of acid-degradability on transfection efficiency was evaluated by investigating the transfection by CSNPs made of 1° monomer with XL, ND1° monomer with XL, 1° monomer with NDXL, and ND1° monomer with NDXL, while proton buffering capacity, zeta potential, and size were kept at similar levels (Blue and pink solid bars and dashed bars in Figure 4). Clearly, all CSNPs made of any nondegradable monomer or crosslinker did not transfect the cells (Figure 4A and B), underscoring the indispensable roles of

acid-degradability in determining transfection. The fact that CSNPs made of ND1° monomer and XL did not transfect the cells indicates that acid-degradability is substantially more crucial than proton buffering capacity for endosomal escape. CSNPs made of nondegradable crosslinker failed to transfect the cells due to limited release of pDNA that is retained in the intertwined polymeric shell.

Improved gene transfection by CSNPs with broadened proton buffering capacity

The utility of the CSNP was made especially apparent for its synthetic flexibility via polymerizing various monomer and crosslinker mixtures at specific molecular ratios. Addition of 10% Im monomer, which has a distinctive dual proton buffering profile (Figure 2), to CSNPs significantly improved transfection efficiency (Figure 2, 3 C, 4 A, and 4B). Surprisingly, adding 30–70% Im monomer reduced the transfection efficiency of CSNPs, while improving the cell viability (Figure 5). To better understand this phenomenon, intracellular trafficking of CSNPs made of 1° monomer, 1° and 10% Im monomers, and 1° and 50% Im monomers was investigated in detail (Figure 6 and 7). When green-labeled pDNA was imaged with red-stained early endosome or lysosome, it was found that all CSNPs efficiently escaped from endosome/lysosome (~90%) in 12 h of incubation (Figure 6). However, more pDNA was found to be still complexed in the polymeric shell of CSNPs made of 1° and 50% Im monomers when green-labeled pDNA and red-labeled polymeric shell co-encapsulation was quantified (Figure 7). A previous study reported a higher transfection by a primary amine- and imidazole-bearing co-polymer than that of a homopolymer of primary amines only.[14] Unlike the observation in this study, the highest transfection was achieved at 50% imidazole content in the previous study, possibly explained by less efficient pDNA complexation by the linear imidazole-containing polymer in a form of a polyplex compared to encapsulation in the crosslinked polymeric shell of CSNPs. The results clearly confirm key design requirements that are indispensable for efficient nonviral vectors, including acid-degradability, broader proton buffering capacity, and free pDNA release upon endosomal escape.

CSNPs for proton buffering-independent endosomal escape

In exploration of a supplementary strategy to the hypothetical proton sponge effect, CSNPs capable of directly disrupting the endosomal/lysosomal membrane was prepared by co-polymerizing TX monomer conjugated with Triton X-100, a commonly used surfactant to lyse cellular membranes or disrupt liposomes (Figure 1A). In its conjugation form to the polymeric network in the shell of CSNPs, Triton X-100 exerts no disruptive effects on the cell membrane. Upon hydrolysis in the endosome, the released free Triton X-100 was hypothesized to assist in the cytosolic release by disrupting the endosomal membrane in addition to the proton buffering by 1° monomer and acid-degradability of all monomers and crosslinker. However, CSNPs made of 2% TX and 1° monomers did not yield enhanced transfection as hypothesized (Figure 5A and B). This is possibly due to the low cellular uptake of CSNPs with a lowered zeta potential (Figure 3A and B) although, once internalized, pDNA were found to be efficiently released into the cytoplasm as hypothesized (Figure 3C). When more than 2% of TX monomer was added, the resulting CSNPs showed detrimental cytotoxicity due to the extensive disruption of endosomal/lysosomal membrane by the rapidly released Triton X-100 (data not shown). The result demonstrated

the possibility of supplementing endosomal escape by a surfactant-conjugated nonviral vector when its molecular ratio is precisely tuned. Harnessing a surfactant that is less extensive in membrane disruption in a gradual manner could be an alternative to TX-100. The curtailed cellular uptake of TX-incorporated CSNPs could also be ameliorated by creating differentially layered polymeric shell with 1° amines on the surface that shields TX, using the high synthetic flexibility.

Conclusion

With the rapid advances in the field of gene therapy, the development of efficient and safe gene delivery vectors has become more important than ever. Understanding the fate of the gene delivery vector once internalized in the cell is of the upmost importance. Proton buffering and acid-degradability are two key theories and play a fundamental role in development of most nonviral vectors. Numerous studies have been conducted to decipher chemical structure-transfection efficiency relationship; however, a more systematic approach that can control for confounding variables is necessary. The CSNP structure is especially advantageous in this aspect. Unlike typical polymer/gene complexes whose stability are variably limited and greatly dependent on the chemical structure of the polymer, the CSNPs provide a stable crosslinked structure that is built from the core surface. The nanoparticle synthesis is simple and flexible as long as individual monomers are prepared, meaning there is no need for polymerization in advance before complexing nucleic acids. Lastly, and most importantly, structure variation is as easy as simply adding the desired molecules into the polymerization mixture.

In conclusion, our core-shell nanoparticles enabled facile, versatile, and highly controlled preparation of NPs consisting of varying monomers and crosslinkers and diverse functionalities via photo-polymerization. This platform allowed for the simple and efficient study of the effect of proton buffering, acid-degradability, and membrane disruption on gene delivery efficiency. Our results indicated that acid-degradability was equally as important as proton buffering and that incorporating both functions significantly improved the transfection efficiency. Moreover, extended buffering capacity achieved by simply mixing monomer with different buffering profile improved the system in instances where efficient dissociation followed upon escape from the endosomal compartments. Addition of Triton X-100 surfactant helped pDNA release from endosomal compartment as hypothesized but indicated the need for further improvement on NP properties such as higher surface charge. Only Im monomer and TX monomers were mixed at different ratios in this study; however, a more comprehensive study, where all 1°, 2°, 3°, Im, and TX monomers are co-polymerized at various ratios, would be a reasonable extension from this study. Moreover, even though other factors such as nanoparticle size were kept at similar level, different cellular uptake resulting from different surface charge of CSNPs greatly impacted the overall transfection efficacy, making it difficult to evaluate the individual influence of proton buffering or acid-degradability during endosomal escape. An additional surface treatment such as PEGylation to unify the surface charge, hence cellular uptake, could answer this question in a subsequent study. Overall, our versatile core-shell nano-system platform proved to be a valuable tool to study the structure-activity relationship in a simple and efficient manner.

Experimental Section

Materials

Protamine sulfate (PS), branched polyethylenimine (PEI, 25 kDa), and 3-(4,5-dimethyl-2-thiazolyl)-2,5-diphenyltetrazolium bromide (MTT) were purchased from Aldrich (Milwaukee, WI). Sodium bicarbonate was purchased from Fisher Scientific (Waltham, MA). Eosin-5-isothiocyanate, Ulysis Alexa Fluor® 488 nucleic acid labeling kit, Alexa Fluor® 555 carboxylic acid succinimidyl ester, nucBlue live cell stain, Image-IT live lysosomal staining kit, and CellLight® early endosomes-RFP were purchased from Invitrogen (Carlsbad, CA). Plasmid DNA (pDNA) encoding enhanced green fluorescent protein (eGFP) (5.0 kbp) was a gift from Dr. Pamela Davis (Case Western Reserve University, Cleveland, OH) and pDNA encoding firefly luciferase (pKCERlucSV, 5.9 kbps) was a gift from Assem Ziady (Case Western Reserve University, Cleveland, OH). Monomers and cross-linkers were synthesized according to previously published method with modifications.[15] HeLa cells were cultured in Dulbecco's modified Eagle's medium (DMEM) (MediaTech, Herndon, VA) with 10% fetal bovine serum (FBS) (Hyclone, Logan, UT) and 1% antibiotics (100 units/mL penicillin; 100 µg/mL streptomycin) (MediaTech).

Core-shell nanoparticle synthesis

Protamine sulfate-eosin conjugate was prepared by reacting 4 mg of protamine sulfate in 2 mL of 10 mM sodium bicarbonate (pH 8.0) with 1 mg of eosin-5-isothiocyanate in 10 µL of DMSO for 3 h at room temperature. Unreacted eosin-5-isothiocyanate was purified using a PD 10 desalting column, changing buffer to de-ionized (DI) water. eGFP-encoding plasmid DNA (20 µg in 500 µL DI water) was added dropwise to 400 µg of PS-eosin conjugate in 500 µL DI water while vortexing. PS/pDNA polyplex was left undisturbed for 30 min to facilitate complexation. After 30 min, 20 mg of monomer in 50 µL of DI water, 4 mg of crosslinker in 50 µL of DI water, and 10 mg of ascorbic acid in 50 µL of DI water were added to the polyplex solution and polymerization was initiated using light irradiation (750 klux) for 15 min on ice bath. Unreacted monomer, crosslinker and ascorbic acid were purified using centrifugal filtration (MWCO 10 kDa, 3500 rpm, 4 °C, 30 min) twice. Resulting core-shell nanoparticles were resuspended in 1 mL DI water for further applications. The size and zeta potential of the nanoparticles were measured using a Malvern Zetasizer Nano ZS (Malvern Instruments, Westborough, MA) at 25°C.

Acid-base titration

The ability of cationic monomers to be protonated and buffer at drop in pH from 11 to 2 was determined by acid-base titration. A greater buffering capacity of a monomer indicates less [H+] in solution and less changes in pH values during HCl titration.[16] Monomer solutions were prepared at 10 mg/mL in 150 mM NaCl and titrated to pH 11 using 1 N NaOH. 2 mL of each solution was titrated with 1 N HCl given in 1 µL increments and pH values were recorded with a pH meter (accumet AB15, Fisher Scientific, Waltham, MA). The buffering capacity (β) was plotted according to $\beta = -dn(H+)/dpH$.

Nanoparticle internalization

Firefly luciferase-encoding pDNA was labeled using an Ulysis Alexa Fluor® 488 nucleic acid labeling kit following the protocol provided by the manufacturer. Core-shell nanoparticles and PS polyplexes encapsulating Alexa Fluor 488-labeled pDNA were prepared as described in the preceding section and incubated with HeLa cells (2×10^4 cells/ well in a 24-well plate) at a concentration of 0.5 μg/mL pDNA. After 4 h of incubation, cells were harvested, washed with cold PBS twice to remove surface-bound nanoparticles and analyzed by flow cytometry. Average fluorescence intensity of the cell was determined as a relative amount of internalized nanoparticles.

In vitro transfection and cytotoxicity assay

HeLa cells were plated at density of 2×10^4 cells/well in a 24-well plate 24 h prior to nanoparticle incubation. Polyplexes and CSNPs at various concentrations in 500 μL of fresh growth media (with 10% FBS) replaced the existing media and the cells were incubated for 4 h at 37°C, followed by replacement with fresh media. After further incubation for 3 days, cells were harvested for flowcytometry analysis using a Guava EasyCyte flow cytometer (Guava Technologies, Hayward, CA). In order to quantify cell viability, cells (4×10^3 cells/ well in a 96-well plate) were incubated in the same manner as 24-well plates. After 24 h of incubation, cytotoxicity was measured by conventional MTT assay.

Confocal microscopy

Core-shell nanoparticles and PS polyplexes encapsulating Alexa Fluor 488-labeled pDNA were prepared as described earlier. HeLa cells were plated at density of 2×10^4 cells/well in a 8-well culture slide (BD Biosciences, Franklin Lakes, NJ) 24 h prior to nanoparticle incubation. Polyplexes and NPs (at a concentration of 0.5 μg/mL pDNA) in 500 μL of fresh growth media (with 10% FBS) replaced the existing media and the cells were incubated for 4 h at 37°C. After 4 h, nanoparticle-containing media were replaced by fresh media and further incubated for 20 h. After total of 24 h incubation, 1 drop of nucBlue Live Cell Stain was added to the media and cells were incubated at room temperature for 20 min, followed by PBS wash twice. Lysosomes were stained by adding 200 μL of 100 nM LysoTracker Red DND-99 in PBS and incubating for 1 min at room temperature, followed by PBS wash twice. Then cells were fixed with 200 μL of 2% p-formaldehyde in PBS for 15 min at room temperature, followed by PBS wash twice.

1°, 1°-10%Im, and 1°-50%Im NP-treated HeLa cells were separately analyzed further by either labeling the shell or labelling early-endosomes. Briefly, the surface of the NPs were mixed with 1 μL of 2 nM Alexa Fluor® 555 carboxylic acid succinimidyl ester at 4°C overnight. Unreacted dyes were removed using a PD-10 desalting column using DI water as eluting solution and incubated with HeLa cells as described earlier. For early-endosome labelling, HeLa cells were incubated with 8 μL of CellLight® early endosomes-RFP (30 particles per cell) for 12 h prior to nanoparticle incubation. After 12 h, 1°, 1°-10%Im, and 1°-50%Im NP-containing media replaced the existing media and the cells were incubated for 4, 12, and 24 h, followed by nucleus staining and fixation as previously described.

Using an Olympus IX2 inverted microscope coupled with a Fluoview 1000 confocal scanning microscopy setup (FV10-ASW) (Olympus America, Inc., Melville, NY), cellular images were observed with a 60×/1.2 NA water immersion plan apochromat objective. Images of Alexa Fluor® 488 were collected using a 488 nm excitation light from a multiple argon laser, a 488 nm dichroic mirror, and a 505–540 nm band pass barrier filter. A 559 nm helium-neon laser, a SMD640 dichroic mirror, and a 575–675 nm band-pass barrier filter were used to obtain the images of Alexa Fluor® 555, LysoTracker Red DND-99, and early endosome-RFP. Images of nucBlue-stained nuclei were acquired using a 405 nm diode laser excitation light, a 405 nm dichroic mirror, and a 430–470 nm band pass barrier filter. Fluorescence images were captured and processed using FV10-ASW 1.6 viewer (Olympus America, Inc.). The cells were scanned in three dimensions as a z-stack of two-dimensional images (1024×1024 pixels) and an image cutting horizontally through approximately the middle of the cellular height was selected to differentiate intracellularly localized polyplexes and nanoparticles from those adsorbed on cellular surface. Each emission light was scanned separately for individual excitations of the dyes to eliminate cross-talk.

Acknowledgements

Data Availability Statement

The data that support the findings of this study are available from the corresponding author upon reasonable request.

References

[1]. Dunbar CE, High KA, Joung JK, Kohn DB, Ozawa K, Sadelain M, Science 2018, 359, eaan4672. [PubMed: 29326244]

[2]. a)Luo D, Saltzman WM, Nat. Biotechnol 2000, 18, 33–37; [PubMed: 10625387] b)Pouton CW, Seymour LW, Adv. Drug Delivery Rev 1998, 34, 3–19;c)Varkouhi AK, Scholte M, Storm G, Haisma HJ, J. Controlled Release 2011, 151, 220–228.

[3]. Li S, Huang L, Gene Ther. 2000, 7, 31–34. [PubMed: 10680013]

[4]. a)Lechardeur D, Verkman AS, Lukacs GL, Adv. Drug Delivery Rev. 2005, 57, 755–767;b)Glover DJ, Lipps HJ, Jans DA, Nat. Rev. Genet 2005, 6, 299–310; [PubMed: 15761468] c) Yin H, Kanasty RL, Eltoukhy AA, Vegas AJ, Dorkin JR, Anderson DG, Nat. Rev. Genet 2014, 15, 541–555. [PubMed: 25022906]

[5]. a)Boussif O, Lezoualc'h F, Zanta MA, Mergny MD, Scherman D, Demeneix B, Behr JP, Proc. Natl. Acad. Sci. USA 1995, 92, 7297–7301; [PubMed: 7638184] b)Murthy N, Thng YX, Schuck S, Xu MC, Fréchet JMJ, J. Am. Chem. Soc 2002, 124, 12398–12399. [PubMed: 12381166]

[6]. a)Benjaminsen RV, Mattebjerg MA, Henriksen JR, Moghimi SM, Andresen TL, Mol. Ther. 2013, 21, 149–157; [PubMed: 23032976] b)Funhoff AM, van Nostrum CF, Koning GA, Schuurmans-Nieuwenbroek NME, Crommelin DJA, Hennink WE, Biomacromolecules 2004, 5, 32–39. [PubMed: 14715005]

[7]. Wang C, Zhao T, Li Y, Huang G, White MA, Gao J, Adv. Drug Delivery Rev. 2017, 113, 87–96.

[8]. a)Hida K, Hanes J, Ostermeier M, Adv. Drug Delivery Rev. 2007, 59, 1562–1578;b)Giacca M, Zacchigna S, J. Controlled Release 2012, 161, 377–388.

[9]. a)Cho SK, Y. J. Kwon, J. Controlled Release 2011, 150, 287–297;b)Cho SK, Pedram A, Levin ER, Kwon YJ, Biomaterials 2013, 34, 10228–10237; [PubMed: 24055523] c) Cho SK, Kwon

YJ, Biomaterials 2012, 33, 3316–3323; [PubMed: 22281425] d)Hong CA, Cho SK, Edson JA, Kim J, Ingato D, Pham B, Chuang A, Fruman DA, Kwon YJ, ACS Nano 2016, 10, 8705–8714. [PubMed: 27472284]

[10]. a)Hartmann L, Börner HG, Adv. Mater. 2009, 21, 3425–3431; [PubMed: 20882508] b)Goldberg M, Mahon K, Anderson D, Adv. Drug Delivery Rev 2008, 60, 971–978;c) Alexis F, Pridgen E, Molnar LK, Farokhzad OC, Mol. Pharm 2008, 5, 505–515. [PubMed: 18672949]

[11]. Pemberton DR, Johnson AF, Polymer 1984, 25, 529–535.

[12]. a)Ghosn B, Singh A, Li M, Vlassov AV, Burnett C, Puri N, Roy K, Oligonucleotides 2010, 20, 163–172; [PubMed: 20565242] b)Benns JM, Choi J-S, Mahato RI, Park J-S, Kim SW, Bioconjugate Chem 2000, 11, 637–645.

[13]. a)Wightman L, Kircheis R, Rössler V, Carotta S, Ruzicka R, Kursa M, Wagner E, J. Gene Med. 2001, 3, 362–372; [PubMed: 11529666] b)Neu M, Fischer D, Kissel T, J. Gene Med 2005, 7, 992–1009. [PubMed: 15920783]

[14]. Wong SY, Sood N, Putnam D, Mol. Ther. 2009, 17, 480–490. [PubMed: 19142180]

[15]. a)Kwon YJ, Standley SM, Goodwin AP, Gillies ER, Fréchet JMJ, Mol. Pharm. 2005, 2, 83–91; [PubMed: 15804181] b)Ko IK, Ziady A, Lu S, Kwon YJ, Biomaterials 2008, 29, 3872–3881. [PubMed: 18585778]

[16]. Cherng JY, J. Pharm. Pharm. Sci. 2009, 12, 346–356. [PubMed: 20067709]
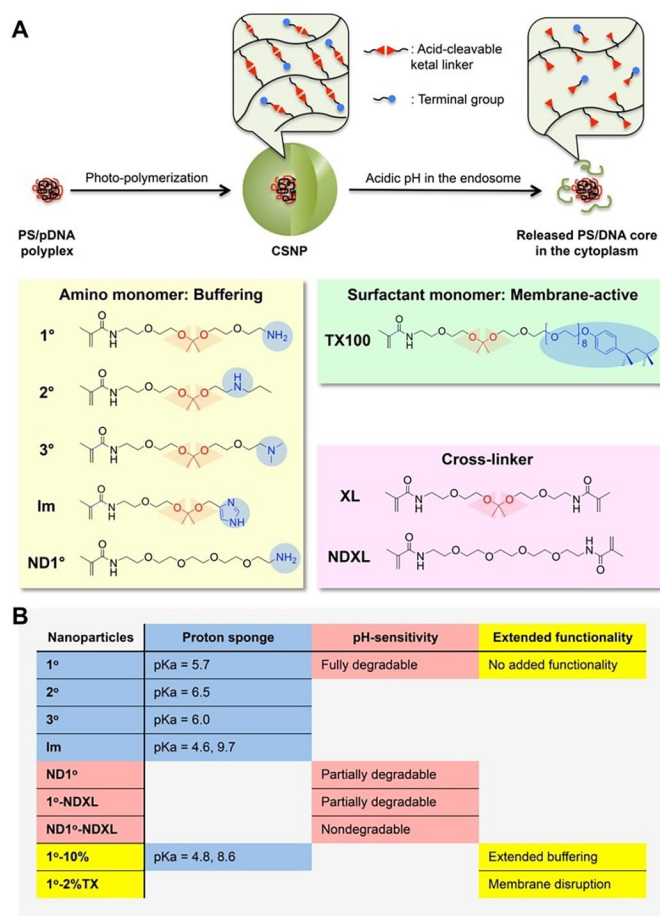
Figure 1.
(A) Synthesis of chemically-tuned CSNPs for molecularly varying proton buffering, acid-degradability, and membrane disruption capabilities via photo-polymerization of 1°, 2°, or 3° amine-, imidazole (Im)-, and Triton X-100 (TX)-bearing monomers with acid-degradable and non-degradable (ND) crosslinkers (XLs) from the surface of eosin Y-tethered PS/DNA polyplex core.
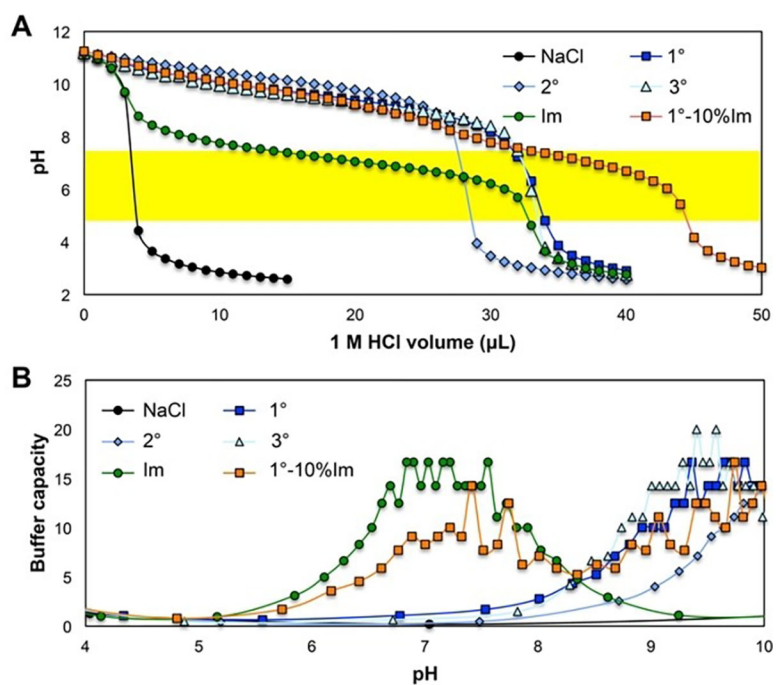
Figure 2.
(A) Acid-base titration and (B) proton buffering capacities of 1°, 2°, 3° and Im monomers in comparison with 1°-10% Im mixture that showed broader, dual proton buffering capacity.
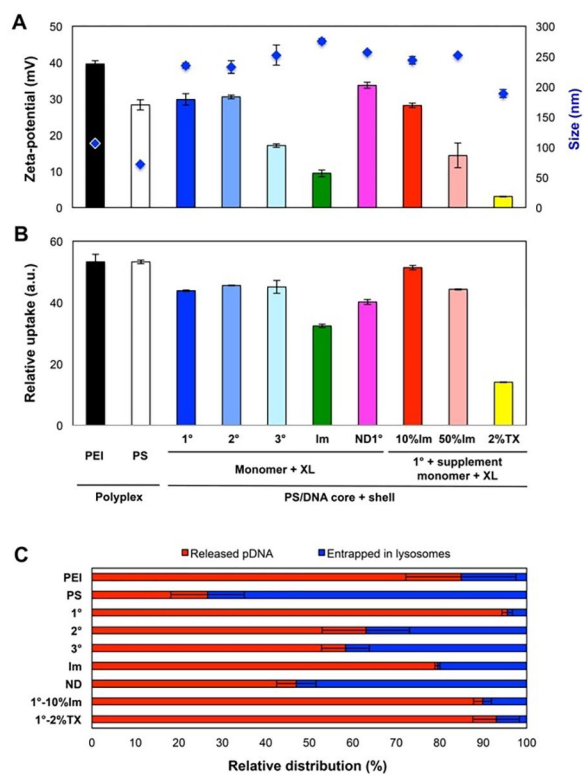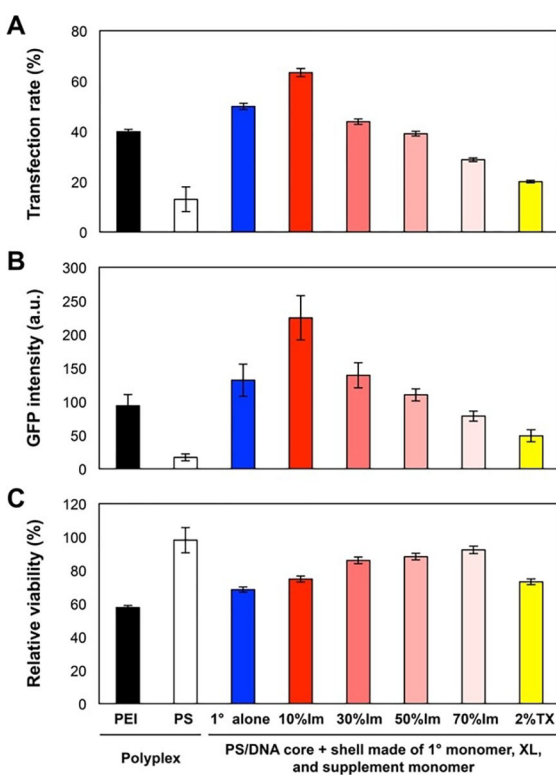
Figure 3.
(A) Surface charge (bars) and size (blue dots) of CSNPs synthesized with varying monomers and crosslinkers listed in Figure 1 (n = 3, mean ± SD). (B) Cellular uptake of CSNPs by HeLa cells (n = 3, mean ±SD). (C) Quantified intracellular distribution of pDNA after 24 h of incubation (n =3, mean ± SD).
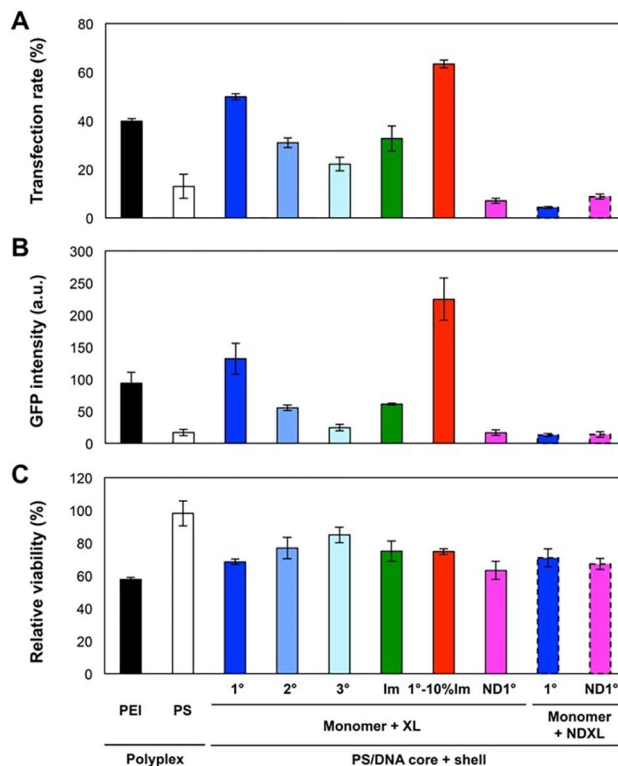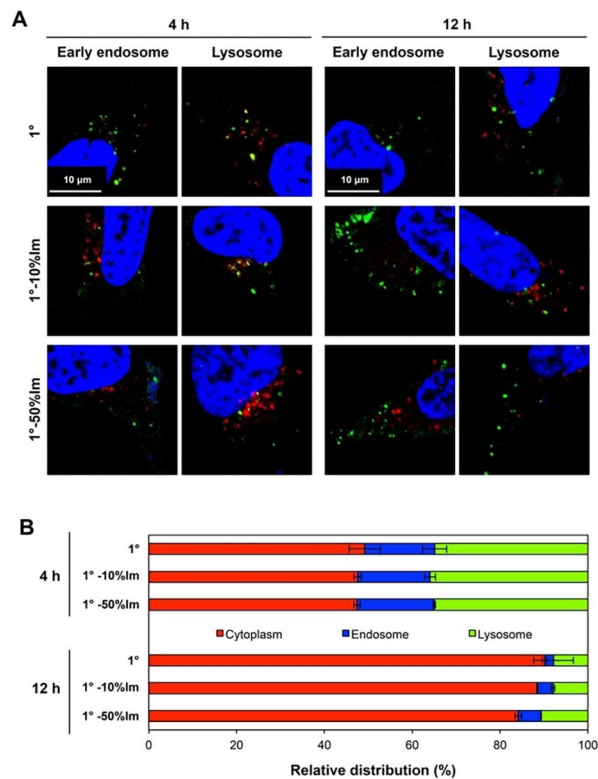
Figure 4.
(A, B) Transfection efficiencies of NPs prepared from monomers showing different buffering capacities and degradability (n = 3, mean ± SD). (C) Relative viability of cells incubated with various nanoparticles (n = 3, mean ± SD).
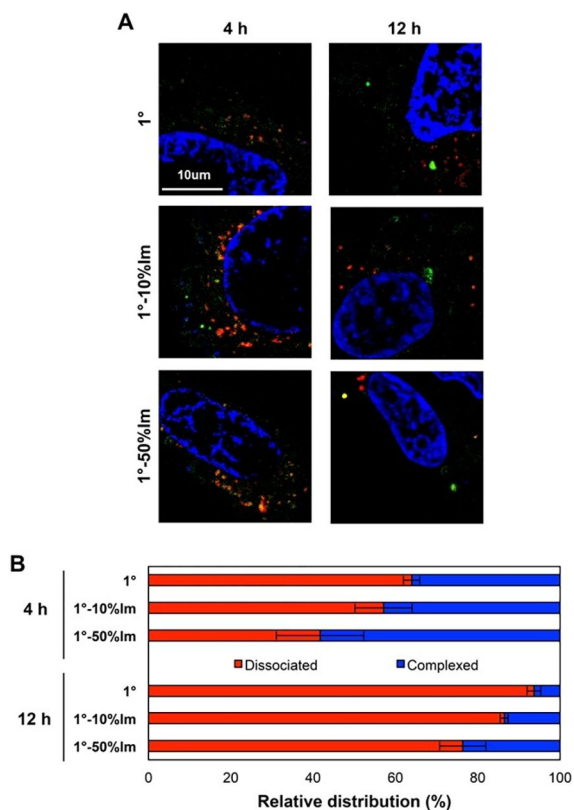
Figure 5.
(A, B) Transfection efficiencies of NPs with additional functionality (Im and TX100 addition) (n = 3, mean ± SD). (C) Relative viability of cells incubated with various nanoparticles (n = 3, mean ± SD).

Figure 6.
(A) Fluorescence confocal images of HeLa cells incubated with CSNPs made of 1°
monomer, 1° and 10% Im monomers, or 1° and 50% Im monomers in their polymeric shell.
Green: AF 488-labeled pDNA; Red: RFP-labeled early endosome (first and third column
images) or lysosome (second and forth column images); Yellow: DNA in the endosomal
compartments; Blue: nucleus. (B) Quantified intracellular distribution of pDNA after 4 and
12 h of incubation (n = 3, mean ± SD).

Figure 7.
(A) Fluorescence confocal images of HeLa cells incubated with CSNPs made of 1°
monomer, 1° and 10% Im monomers, or 1° and 50% Im monomers. Green: AF 488-labeled
DNA; Red: AF 555-labeled polyketal layer; Yellow: complexed DNA in CSNPs; Blue:
nucleus. (B) Quantified dissociation of pDNA from CSNPs after 4 and 12 h of incubation (n
= 3, mean ± SD).